ISBN: 978-3-95450-168-7 doi:10.18429/JACoW-IPAC2015-THPF134

MAGNET DESIGN AND SYNCHROTRON DAMPING CONSIDERATIONS FOR A 100 TeV HADRON COLLIDER*

S. Assadi, D. Chavez, J. Gerity, T. Mann, P. McIntyre#, N. Pogue[1], A. Sattarov,
Texas A&M University, College Station, TX 77845, USA
M. Tomsic, Hypertech, Columbus, OH 43228 USA

Abstract

A conceptual design is presented for a 100 TeV hadron collider based upon a 4.5 T NbTi cable-in-conduit dipole technology. It incorporates a side radiation channel to extract synchrotron radiation from the beam channel so that it does not produce limitations from heating on a beam liner or gas load limits on collider performance. Synchrotron damping can be used to support 'bottom-up' stacking to sustain maximum luminosity in the collisions.

INTRODUCTION

The importance of extending searches for new gauge fields by another order of magnitude has led to the suggestion by CERN to develop a Future Circular Collider (FCC) that could contain a 100 TeV hadron collider [1]. We report on development of a particular design for such a collider, motivated by a systematic optimization of its two major cost drivers – the dual ring of superconducting magnets and the tunnel. The two drivers optimize oppositely as a function of the choice of magnetic field.

The tunnel cost depends strongly upon the choice of site for the collider. An optimum case was the siting of the SSC near Dallas, for which the actual cost for the 39 km of completed 4 m diameter tunnels was \$3,300/m (1992). The advance rate for the tunnels averaged 40 m/day, the fastest rate of advance on any recorded large-bore tunnel project in history [2]. The favourable cost was the result of a favourable choice of rock: the Austin Chalk and Taylor Marl formations permit rapid excavation using tunnel boring machines and are self-supporting so that lining can be installed in coordination with excavation schedule [3].

The same site could accommodate a circular tunnel up to 270 km circumference and still remain entirely within those favourable rock strata. A 270 km circumference would require B_0 ~4.5 T to produce hadron collisions at 100 TeV. The tunnel cost today for a 100 TeV collider can be estimated from the SSC tunnel costs using the Construction Cost Index [4]: (270 km)(\$3,300/m)(2.04) = \$1.8 billion. Since this cost is almost certainly less than that of a superconducting magnet ring, it is reasonable to take 270 km as a working choice for collider design and to optimize the design of a superconducting dipole suitable for 4.5 T operating field.

*Work supported by the George and Cynthia Mitchell Foundation.
[1] current address PSI, Villigen, Switzerland.
#mcintyre@physics.tamu.edu

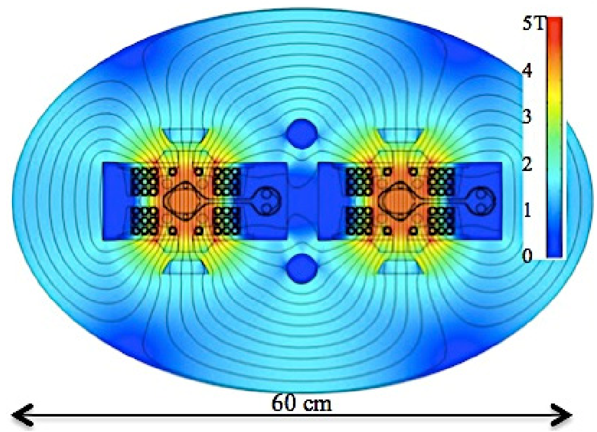

Figure 1: 4.5 T dipole for 100 TeV hadron collider.

4.5 T CABLE-IN-CONDUIT DIPOLE

Figure 1 shows the magnetic design of a 4.5 T dual dipole suitable for use in a 100 TeV hadron collider. The design uses a block winding of round NbTi cable-in-conduit (CIC). The design is inspired by the simplicity of the CIC dipoles that were developed at JINR for use in SIS-100 and FAIR [5]. Each dipole is configured in a C geometry so that the horizontal fan of synchrotron radiation exits the beam tube through a slot aperture and is absorbed in a separately cooled radiation channel as shown in Figure 2.

The main parameters of the dipole are summarized in Table 1. For a dipole field strength of 4.5 T, the C geometry shown requires no more superconductor than would a conventional dipole. A main benefit of the CIC conductor is that it simplifies the fabrication and support of end windings, as shown in Figure 2.

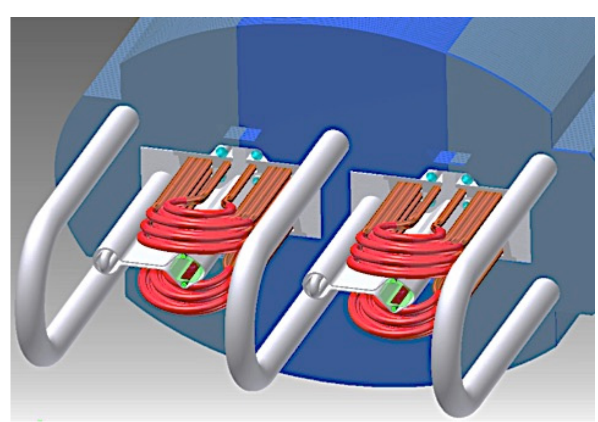

Figure 2: View of end windings in the CIC dipole.

ISBN: 978-3-95450-168-7 doi:10.18429/JACoW-IPAC2015-THPF134

Table 1: Main Parameters of the CIC Dipole

Operating bore field	4.5	T
# turns	20	
NbTi/Cu wire diameter	1.2	mm
Operating current	20	kA
Short-sample bore field	5.0	T
physical aperture	3.5x2.5	cm²
Dipole length	20	m
Inductance	0.3	mH/m
Stored energy	63	kJ/m
LHe flow in windings	32	cm³/s
Operating temperature	4.2-4.3	K
Max temp in quench	115	K

The windings for each dipole are fabricated from two lengths of the CIC conductor, shown in Figure 3, following the structured cable method originated by McIntyre [6]. The CIC conductor is fabricated by cabling strands of NbTi/Cu superconductor onto a spring tube, and spiral-wrapping a thin stainless steel tape that provides a slip surface. The cable then passes through a continuous tube-forming (CTFF) process [7] in which a strip of Monel alloy is rolled to form an open-seam tube around the cable (Figure 4a), and the seam is closed and laser-welded to form the outer sheath. The sheath is then drawn down onto the cable to load the strands into compression against the spring tube so that they are immobilized. The drawing results in highly reproducible cable dimension, which is critical for controlling homogeneity in the magnetic design. A method has been validated by which the bend radius for required for end windings can be made while keeping interior regisration of the cable intact (Figure 4b).

The magnetic design would support 5.0 Tesla short-sample field at 4.5 K with 20 kA coil current. Figure 5 shows the calculated systematic multipoles in the magnetic design as a function of field. All multipoles are $b_n < 10^{-4}$ cm^{-n} over the range of field from injection to collision energy.

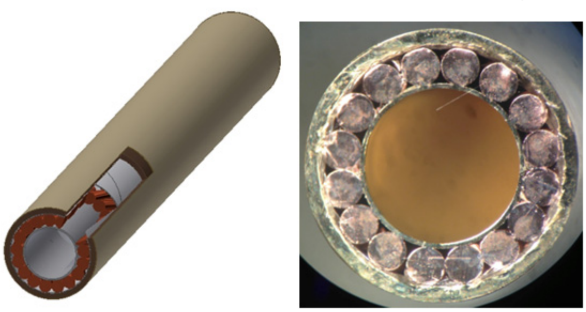

Figure 3: Cable-in-conduit conductor.

Figure 4: a) Continuous tube forming of the sheath tube; b) specimen of CIC cable bent to the radius required for the windings of the 4.5 T dipole.

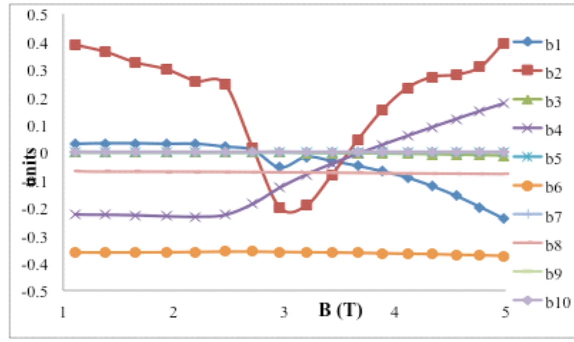

Figure 5: Calculated multipoles *vs.* bore field.

Coil Positioning and Stress Management

All strands must be supported within the cables so that they cannot move under Lorentz forces during operation. The mechanical support is provided by the stress management that is integrated into the CIC conductor itself. Within the cable the sheath acts as a stress bridge and the spring tube provides a soft-modulus loading to protect the wires inside from being strained [6]. Figure 6a shows the calculated von Mises stress that is produced when the sheath is compressed onto the cable so that each strand just dimples the spring tube. The sheath and the spring tube deform under local elastic compression, but the strands themselves are immobilized with very little internal stress.

The one-piece lamination stack is designed to provide bridging support to prevent coil motion under Lorentz stress, particularly the vertical forces compressing upon the slot aperture between beam tube and radiation channel. Figure 6b shows the calculated von Mises stress when the dipole is energized to 4.5 T. The maximum displacement of any superconducting strand is 25 µm.

Cryogenic and Vacuum Design

Supercritical helium flows readily through the open spring tube within all windings during magnet operation, and bathes the strands. In the event of a microquench within one strand the He enthalpy is directly available to heal the microquench so that it

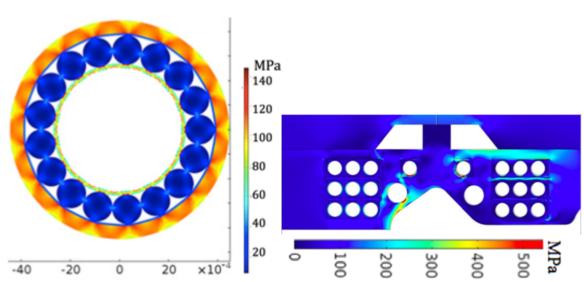

Figure 6: Stress distributions a) within the CIC conductor after drawing; b) in the epoxy-impregnated upper half-winding of the CIC dipole at 4.5 T field.

ISBN: 978-3-95450-168-7 doi:10.18429/JACoW-IPAC2015-THPF134

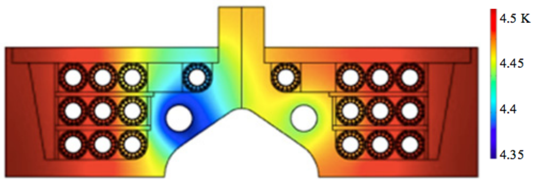

Figure 7: Simulation of heat transfer within the winding, assuming 0.4 W/m/bore distributed in a 1/r distribution, He velocities of 0.15 m/s in the spring tubes and 0.5 m/s in the central He flow channels.

does not propagate.

The radiation channel contains NEG vacuum pumping and is cooled at ~150 K by separate cooling tubes so the ~20 W/m/bore of synchrotron radiation heat can be removed without major power requirement.

By separating the heat from synchrotron light and the associated gas desorption from the beam tube, we remove their effects upon the circulating beam that could otherwise limit the achievable luminosity [8].

The dynamic heat load due to continuously lost particles from inelastic beam-gas scattering during high-luminosity collider operation has been scaled based on measurements during the 2012 LHC operation [9]:

$$Q = Q_0 \cdot \frac{N}{N_{LHC}} \cdot \frac{n}{n_{LHC}} \cdot \frac{E}{E_{LHC}} \cdot \frac{\rho}{\rho_{LHC}} = .4\, W/m/bore$$

where $Q_0 = 0.024 W/m/bore$ is the dynamic heat load due to inelastic scattering at LHC. The heat transfer to the supercritical helium flow in the CIC cable has been simulated, as shown in Figure 7. The heat load Q can be removed while keeping the maximum temperature in the windings to 4.5 K.

Quench Protection

The method of driving quench in the cable is to externally heat a ~10 cm segment of cable using heater foils bonded to the outside of the sheath at one end of each turn. We have simulated quench propagation in the windings at various operating fields, in which current is delivered to the heaters beginning 10 ms after quench initiation. Quench propagation was simulated through the 10 m lengths of cable to the dipole mid-point. The quench event has a maximum 21 MIITS, and the highest temperature reached in the winding is 216 K. The heater power needed to drive quench in one U-bend is 600 W.

SYNCHROTRON-DAMPING

The beam dynamics in a 100 TeV hadron collider is dominated by synchrotron radiation, which damps the beam emittances on the time scale of a collider run. Following Keil's analysis [10] of the dynamics of a synchrotron-radiation-dominated hadron collider, the luminosity L and the total synchrotron radiation power P can be related directly to the total number of protons N, the β_x at the collision point, and the allowable tune shift ξ:

$$L = \frac{\gamma \xi N f}{\beta_x r_p} \quad P = \frac{8\pi}{3}\frac{Nfre^2}{R}\gamma^4 \quad L = \left(\frac{3\xi}{8\pi\gamma^3 \beta_x r_p e^2}\right) PR$$

For a given total synchrotron radiation power, the achievable luminosity increases in proportion to collider circumference. Also the synchrotron heat per meter deposited in the superconducting magnets for a given luminosity decreases inversely with R^2.

We have simulated the time evolution of the transverse emittance, intensity, and the luminosity in a lattice similar to that of the SSC [11]. Figure 8 shows the simulation during a store. Note that the synchrotron damping collapses the transverse emittances and compensates for the loss of protons from collisions so that the luminosity actually increases with time. RF heating is used to maintain ~constant longitudinal emittance even as it is damped by synchrotron radiation in order to control instabilities.

The damping of transverse emittance opens the possibility to use 'bottom-up' stacking of fresh beam to periodically refresh the store and maintain maximum luminosity ~indefinitely. In this approach the store is paused, the low-beta squeeze is relaxed, the beam is collimated and decelerated to the 15 TeV injection energy. A fresh filling of bunches is momentum-stacked with the stored beam using one of several conventional methods for momentum-stacking [12].

The momentum acceptance of the collider is ΔE/E = $5x10^{-4}$, which is adequate for momentum-stacking. The stacked beam is then re-accelerated, the low-beta squeeze is applied, and collisions resume. In this manner it should be possible to sustain a luminosity that is actually greater than the initial single-filling luminosity for an indefinite time with >90% of the time available for colliding beam physics.

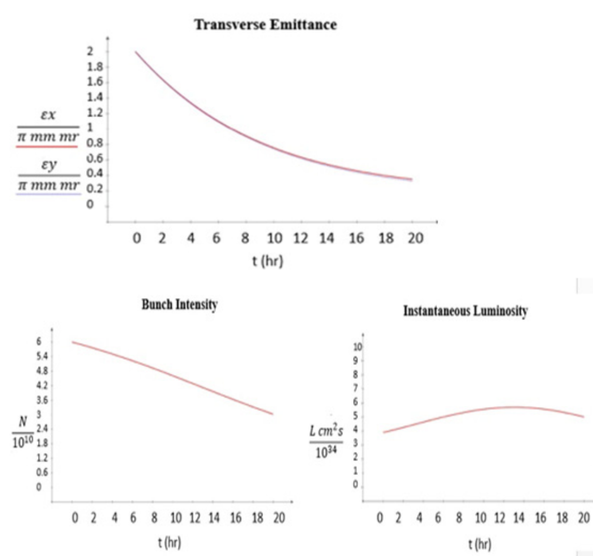

Figure 8: Time evolution of transverse emittance, intensity, and luminosity during a store, including effect of synchrotron damping.

ISBN: 978-3-95450-168-7 doi:10.18429/JACoW-IPAC2015-THPF134

REFERENCES

[1] Future Circular Collider Study Kickoff Meeting, Geneva, Feb. 12-14, 2014, http://indico.cern.ch/event/282344/timetable/#20140212

[2] Robbins Co., TBM Performance World Records, http://www.therobbinscompany.com/en/news-events/world-records/

[3] P. Nelson, 'Geology and geotechnical considerations of the SSC site in Texas: tunneling and construction at the Dallas-Ft. Worth SSC site', (1989). http://lss.fnal.gov/archive/other/ssc/ssc-n-620.pdf

M. Werner *et al.*, 'Bedrock geology of the SSC site', SSC report SSC-GR #65, (1990). http://lss.fnal.gov/archive/other/ssc/ssc-sr-1124.pdf

[4] Eng. News Record, Construction Cost Index 1908-2015,http://enr.construction.com/economics/historical_indices/construction_cost_index_history.asp

[5] E. Fischer *et al.*, 'Superconducting SIS100 prototype magnets', IEEE Trans. Appl. Supercond. **20**, 3, 218 (2010). http://ieeexplore.ieee.org/stamp/stamp.jsp?arnumber=05443653

[6] P. McIntyre, A. Sattarov, and R. Soika, 'Armored spring-core superconducting cable and method of construction', U.S. Patent 6,448,501 B1 (2002). http://www.google.com/patents/US6448501

[7] M. Tomsic, 'Method for manufacturing MgB_2 intermetallic superconductor wires', US Patent 6,687,975 (2004). http://www.google.com/patents/US6687975

D.D. Doll *et al.*, 'Method for continuously forming superconducting wire and products therefrom', Patent WO2014109803 A2 (2014). http://www.google.com/patents/WO2014109803A2?cl=en

[8] R. Kersevan, 'Synchrotron radiation & vacuum concepts', Future Circular Collider Study Kickoff Meeting, Geneva, Feb. 12-14, 2014, https://indico.cern.ch/event/282344/session/2/contribution/25

[9] L. Tavian, 'Performance limitations of the LHC cryogenics: 2012 review and 2015 outlook', LHC beam operation workshop, Evian 2012, http://cds.cern.ch/record/1562028/files/CERN-ATS-2013-045.pdf?version=1, p. 129.

[10] E. Keil, 'Synchrotron radiation dominated hadron colliders', Proc. 1997 Part. Accel. Conf., http://accelconf.web.cern.ch/accelconf/pac97/papers/pdf/7P007.PDF

[11] M.J. Syphers, 'Evolution of SSC Lattice Design', PAC 1991. https://accelconf.web.cern.ch/accelconf/p91/PDF/PAC1991_0117.PDF

[12] P.S. Yoon, D.P. McGinnis, and W. Chou, 'The modeling of RF stacking of protons in the Accumulator', FERMILAB-TM-2361-AD (2005), http://lss.fnal.gov/archive/test-tm/2000/fermilab-tm-2361-ad.pdf

A nice animation of momentum stacking is given at http://wwwap.fnal.gov/~syoon/SC/rf_stack_4_lsc_anim.gif